



A Westerbork Radio Telescope for GNSS Signal In Space Monitoring

A. van Ardenne⁽¹⁾, Hans van der Marel⁽¹⁾, Andre Bos⁽²⁾ and Koos Kegel⁽¹⁾

(1) ASTRON, Oude Hoogetveensedijk 4, 7991PD Dwingeloo, The Netherlands, <http://www.astron.nl>

(2) Science and Technology B.V., Olaf Palmestraat 18, Delft, The Netherlands

Abstract

With the increasing reliance on accurate and trustworthy use of GNSS data, there is an increased need to have access to a correct, optimized and continuously operating set of reference systems to support the GNSS operational system. In Europe, the advent of the Galileo system [1], induced an early need for insightful data starting from the launch of Giove A and B as the first prove of concept satellites for the Galileo system. In response to this, several European private and public parties shared development capabilities to arrive at a Signal In Space (“SIS”) monitoring facility for this purpose. In the Netherlands the thorough knowledge and capabilities of the Westerbork Synthesis Radio Telescope (WSRT) used for Radio Astronomy supported this and further developments. In the present contribution, key system aspects of the dedicated facility at the WSRT are detailed for this and further developments for GNSS usage.

1. Introduction

In the first decade of this millennium, Europe started to build its own GNSS system called Galileo. Aimed to be ready in this decade, it will consist of 28 satellites of which 22 have been launched successfully so far.

Leading up to this, preparations started in 2007 to suitably modify one telescope out of the 14 of the Westerbork Synthesis Radio Telescope (“WSRT”) array [2] in order to support the early assessment of the Galileo system in the In Orbit Validation phase. While preparations continued, a contract was awarded through the European Space Agency in the end of 2008 to develop a Signal In Space monitoring system for observations on the early Galileo test satellites Giove A and B [3] and the first 4 flight models of the Galileo satellites.

This Signal Monitoring Facility (“SMF”) system was initially using telescope 6 with a suitably modified multifrequency frontend receiver [e.g. 4] to allow for the required calibration and circular polarization observations for GNSS usage.

As very stringent requirements called on the accurate calibration of group-delay and absolute power levels, the telescope apex was equipped with a suitable comb generator [5]. Furthermore, a new “software” receiver allowed for the SIS performance analysis. This resulted in

the successful qualification in early 2014 at the onset of further Galileo satellites in the next phase.

Through this success, further developments lead to a new prototype wideband receiver and successful negotiations with the European GNSS Agency (“GSA”). This facilitated the move of the facility to another telescope (“0”) of the WSRT less used for radio astronomy purposes.

2. System Layout

The principle system layout is given in Figure 1 below depicting the relation between the SIS monitoring and analysis receiver which functionality is largely software PC-based.

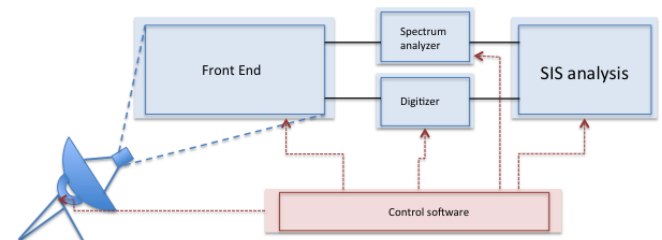


Figure 1. Principle system block diagrams. The default High Gain Antenna is Telescope 0, with Telescope 1 as fall back. A duplicate cooled receiver allows for redundancy.

Table 1 summarizes pertinent data of the telescope used for the GNSS observations using a modified cryogenically cooled receiver. The telescope includes a comb generator in the apex for accurate group-delay calibration.

Table 1. Pertinent data describing the High Gain Antenna.

Antenna type	25m High gain antenna, equatorial mount, prime focus
Antenna gain	48 dBi @ 1.2GHz
Polarization	RHCP/LHCP or X/Y
Frequency range	1.12-1.65 GHz
Instantaneous bandwidth	160 MHz
Half-beam width	0.5 deg.
Pointing accuracy	0.005 deg.
Slew rate	18 deg./min
System temperature	25 K
Calibration	Apex comb generator

Figure 2 presents the full SMF system in more detail depicting the left-/right-hand circular outputs from the HGA. Other instruments are for RF monitoring and data analysis, storage and -user distribution.

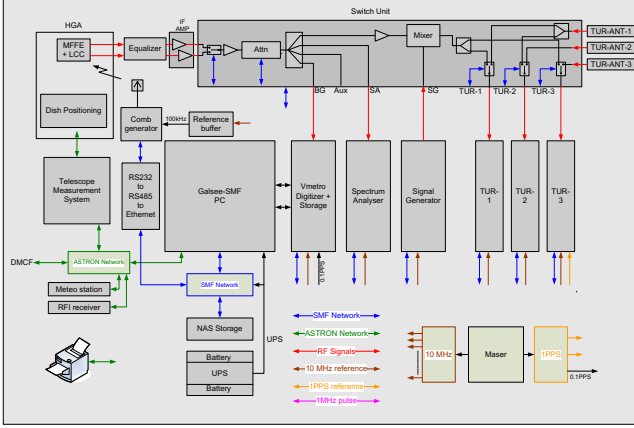


Figure 2. Detailed block diagram of the full SMF system. The full post-processing analysis is done in the SIS PC-based receiver after 8-bit digitization at 400Ms/sec. over max. 160MHz bandwidth. Note that the TURs were removed from the system after completion of the IOV phase.

In the present system, the maximum observable bandwidth of 160 MHz allows to simultaneously observe and analyse the Galileo specific E5+E6 (1145-1300MHz) bands and the E1 (1554-1596MHz) band separately.

While the very low system noise is not strictly necessary, its proven advantage is the very high dynamic range observation of the Galileo spectra allowing to analyse the signal spectral purity to a high degree.

With some sensitivity compromise, a new uncooled and dedicated wideband receiver is now being developed, allowing for the coherent observation of all Galileo bands besides those of other, GNSS satellites, in one go. This dedicated wideband receiver makes use of a special frequency mixing scheme to gain experience in coherent spectra reception and data analysis without affecting the digital back-end. A next receiver architecture will be designed such that the complete 500MHz frequency band can be analyzed.

3. Calibration

3.1 Gain calibration

The receiver antenna pattern is calibrated using holographic measurements on radio astronomical sources. From these measurements, the antenna pattern is characterized in detail from which the efficiency and pointing errors are determined.

The absolute gain of the receiver chain is calibrated using strong astronomical radio sources of which the spectral power flux density at the Earth is accurately known.

Measurements have shown that the stability of the gain of the receiver chain is better than 0.06 dB over a period of 8 hours.

3.2 Phase calibration

As the WSRT is usually used as an interferometer, it has been demonstrated that the phase stability (obtained from astronomical measurements) is better than ± 4 degrees over a period of 12 hours. However, due to the fact that all telescopes in the interferometer have the same properties, it is not possible to use these measurements to calibrate the frequency-dependent group delay or phase properties of the receiver chain.

The method used for the frequency dependent broadband phase calibration is described in [5] in detail of which a summary is given here.

The impulse response of a filter or a receiver chain is the Fourier transform of the transfer function of the filter or receiver chain. The spectrum of a pulse is wide and its phase is well defined. Therefore, pulses are very well suited for the calibration of a receiver chain with a large instantaneous bandwidth. Frequency conversions in the receiver chain do not have an impact on the analysis. A repetitive pulse generator, or comb generator, can be used for accurate pass-band calibration, both in amplitude and phase.

If a Dirac delta function is represented by $\delta(t)$, then a periodic impulse train is given by

$$x(t) = \sum_{k=-\infty}^{+\infty} \delta(t - kT) \quad (8)$$

This signal is periodic with fundamental period T . The Fourier transform of this signal is

$$X(\omega) = \frac{2\pi}{T} \sum_{k=-\infty}^{+\infty} \delta\left(\omega - \frac{2\pi k}{T}\right) \quad (9)$$

again an impulse train, but now in frequency with fundamental period $\omega = 2\pi/T$. As the spacing between the impulses in time gets longer, the spacing between impulses in frequency gets smaller. When observed on a spectrum analyser, these appear as a “comb” of “spikes”.

In the ideal case the periodic signal consists of a repetition of Dirac delta pulses. However, practical implementations of an impulse generator have a finite bandwidth, thus producing an impulse with a finite length. Let $p(t)$ be the shape of the pulse as a function of time and $h(t)$ the impulse response of the receiver chain. Then the signal $z(t)$ that is measured at the end of the receiver chain is a convolution of the impulse train, the pulse shape and the impulse response and is represented by

$$z(t) = h(t) * p(t) * x(t) \quad (10)$$

In the frequency domain these are multiplications:

$$Z(\omega) = H(\omega) \cdot P(\omega) \cdot X(\omega) \quad (11)$$

in which $H(\omega)$ is the (complex) transfer function of the receiver chain. Using Eq. 11 the inverse of the transfer function $1/H(\omega)$ can be computed from which a deconvolution filter can be determined.

In the case of Gaussian shaped pulses (as most impulse generators intend to produce) the bandwidth BW is related to the $FWHM$ of the pulse width τ_{pulse} according to the following equation:

$$BW = \frac{1}{\tau_{pulse}} \quad (12)$$

As the pulses occur repetitively, the signal-to-noise ratio of the estimated transfer function can be improved by combining multiple pulse periods. This can be achieved by averaging pulse periods, or by correlation of the time series with an ideal Dirac impulse train (as in Eq. 8). These operations yield identical results. However, for both cases it is important that all pulses arrive exactly at the expected times. Therefore, the time jitter in impulse generation and in recording should be as small as possible. The impulse generator and the ADC should be synchronized to the same (stable) clock, to create a locked system.

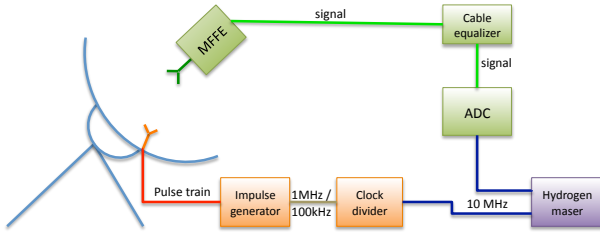


Figure 3. Schematic overview of the phase calibration set-up

Figure 3 schematically shows the phase calibration set-up as used in the GALSEE SMF system at the WSRT. The heart of the set-up consists of an Avtech AVH-S-1-B impulse generator, which produces near-Gaussian shaped pulses with a width of ~ 130 ps. The impulse generator, ADC and mixers in the receiver chain are all locked to the same 10 MHz clock signal, coming from an active hydrogen maser. The output of the impulse generator is connected to a conical log-spiral antenna which emits the calibration signal with the same polarisation as the satellite signal.

The accuracy with which the phase of the band pass can be determined is $\pm 0.3^\circ$ and for the amplitude an accuracy of better than ± 0.05 dB can be obtained. These numbers have been obtained during repeating measurements over a period of 8 hours, which shows that both the impulse generator and the receiver chain are very stable.

4. Measurement analyses

As described in the introduction of this paper, the analyses is performed by a software receiver schematically shown in Figure 4. The received data is being sampled by a high-speed data sample, and the stored data is being processed to perform a number of analyses, including –but not restricted to– the estimation of the Power Spectral Density (PSD) of the signal, the estimation of the Doppler-shift, signal demodulation, power estimation, and the constellation diagram.

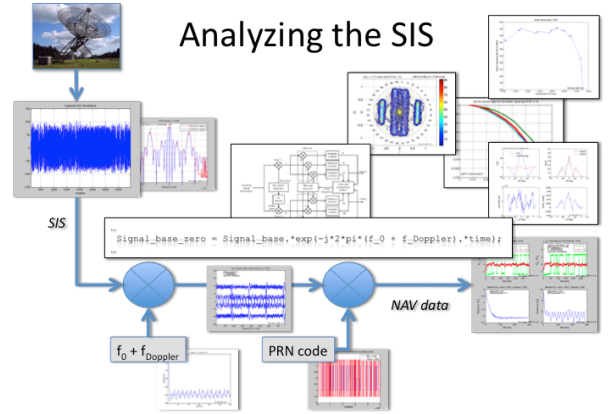


Figure 4. Schematic structure of the signal analyses method.

An example the PSD of the E1 signal of Galileo is given in the following figure 5. Some additional analyses are being made as well, such as the comparison with the theoretical PSD, and the estimation of imbalances in the PSD by comparing the amplitude of the main lobes of the PSD

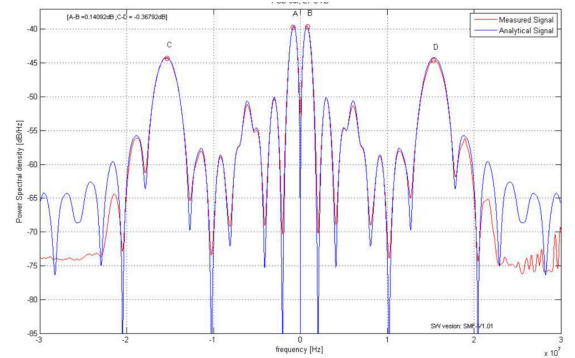


Figure 5. PSD as measured by the WSRT system, including comparison of the measured signal with the theoretical PSD.

5. Summary

We demonstrated that with adequate modifications including dedicated phase and amplitude calibration and the development of the Signal in Space receiver, a radio telescope of the Westerbork array could successfully be employed for high performance GNSS monitoring. With

some sensitivity compromise, the development of a wider band uncooled digital receiver instead of the relatively complicated multifrequency front end, holds promise for a highly flexible next step.

6. Acknowledgements

The team acknowledges the collaborative support from ESA and Thales Alenia Space (It.) in the IOV phase, the Netherlands Space Office, the European GNSS Agency and supporting colleagues from the ASTRON and S&T staff.

7. References

1. http://www.esa.int/Our_Activities/Navigation/Galileo/What_is_Galileo
2. <https://www.astron.nl/radio-observatory/public/public-0>
3. <http://www.esa.int/esapub/br/br251/br251.pdf>
4. G.H. Tan, "Upgrade of the Westerbork synthesis radio telescope: The multi frequency front end", *Proc. 26th European Microwave Conf.*, September 1996, p59-64.
5. J. van der Marel and A. Bos, "Broadband Phase Calibration of a High Gain Antenna", *Proc. of the 32nd ESA Workshop on Antennas for Space Applications*, October 2010.